



Correlating geochemistry, tectonics, and volcanic volume along the Central American volcanic front

Louise L. Bolge

Lamont Doherty Earth Observatory, Earth Institute at Columbia University, 61 Route 9W, Palisades, New York 10964, USA (bolge@ldeo.columbia.edu)

Michael J. Carr

Department of Earth and Planetary Sciences, Rutgers University, 610 Taylor Road, Piscataway, New Jersey 08904, USA

Katherine I. Milidakis

Department of Earth Sciences, Boston University, 675 Commonwealth Avenue, Boston, Massachusetts 02215, USA

Fara N. Lindsay and Mark D. Feigenson

Department of Earth and Planetary Sciences, Rutgers University, 610 Taylor Road, Piscataway, New Jersey 08904, USA

[1] The Central American volcanic front consists of several distinct volcanic lineaments or segments, separated by right steps and/or changes in strike. Each volcanic line is rotated slightly counterclockwise from the strike of the inclined seismic zone. Right stepping volcanic lines, oblique to the strike of the slab, create a sawtooth pattern in the depth to the slab. Zr/Nb is the first geochemical signature with consistent large offsets at the right steps in the volcanic front. Moreover, Zr/Nb mirrors the sawtooth variation in depth to the slab; within a segment it increases from SE to NW, and at the right steps, separating segments, it abruptly decreases. Unfortunately, there is no simple negative correlation between Zr/Nb and depth to the slab because Zr/Nb also has a regional variation, similar to previously documented regional variations in slab tracers in Central America (e.g., Ba/La, U/Th, and $^{87}\text{Sr}/^{86}\text{Sr}$). Within a segment, Zr/Nb decreases with increasing depth to slab. This can be explained in two ways: a Nb retaining mineral, e.g., amphibole, in the subducting slab is breaking down gradually with increasing depth causing more Nb to be released and consequently a smaller Nb depletion in deeper melts; alternatively, all melts have the same initial Nb depletion which is then diluted by acquiring Nb from the surrounding mantle wedge as melts rise and react. Deeper melts have longer paths and therefore more reaction with the mantle wedge diluting the initial Nb depletion. Within each volcanic segment there is variation in eruptive volume. The largest volcanoes generally occur in the middle of the segments, and the smaller volcanoes tend to be located at the ends. Connecting the largest volcanoes in each segment suggests an axis of maximum productivity. This is likely the surface projection of the center of the melt aggregation zone. The largest volcanoes tap the entire melt zone. Those with shallow depths to the slab tap just the front part of the melt zone and have very large Nb depletions. Those at greater depths tap the back part of the melt zone and have much smaller Nb depletions.



Components: 9557 words, 10 figures, 1 table.

Keywords: HFSE; Central America; Nb; Zr; subduction.

Index Terms: 1031 Geochemistry: Subduction zone processes (3060, 3613, 8170, 8413); 3613 Mineralogy and Petrology: Subduction zone processes (1031, 3060, 8170, 8413); 8170 Tectonophysics: Subduction zone processes (1031, 3060, 3613, 8413).

Received 24 June 2009; **Revised** 22 October 2009; **Accepted** 29 October 2009; **Published** 24 December 2009.

Bolge, L. L., M. J. Carr, K. I. Milidakis, F. N. Lindsay, and M. D. Feigenson (2009), Correlating geochemistry, tectonics, and volcanic volume along the Central American volcanic front, *Geochem. Geophys. Geosyst.*, *10*, Q12S18, doi:10.1029/2009GC002704.

Theme: Central American Subduction System

Guest Editors: G. Alvarado, K. Hoernle, and E. Silver

1. Background

[2] The Central American volcanic front has several characteristics that have made it a focus for geochemical studies of arc volcanism [e.g., Hoernle *et al.*, 2008; Carr *et al.*, 2007a, 2007b; Gill *et al.*, 2006; Feigenson *et al.*, 2004; Carr *et al.*, 2003]. Recently, the most commonly remarked feature is the large regional variation in several element and isotope ratios thought to trace fluids derived from the subducted slab, e.g., Ba/La and $^{87}\text{Sr}/^{86}\text{Sr}$ [Carr *et al.*, 1990]. However, the distinct feature of the Central American volcanic front that was first recognized is the remarkable distribution of the volcanoes into several distinct lineaments [Dollfus and Montserrat, 1868; Sapper, 1917]. These lineaments, called volcanic segments by Stoiber and Carr [1973], divide the front into seven segments separated by right steps and/or changes in strike (Figure 1a). Carr *et al.* [2007b] summarized the largely unsuccessful attempts to find geochemical variations that reflect these structures. Although offset volcanic lines are present in other convergent margins, the lines in Central America are unusual in being distinct, consistently right stepping and commonly associated with areas of extension such as the Gulf of Fonseca, Lake Managua and Lake Nicaragua (Figure 1a) [Stoiber and Carr, 1973]. The origin of the volcanic segmentation has been controversial. Stoiber and Carr [1973] proposed the segments reflected structures in the subducting plate; offsets in the subducting slab and vertically rising conduits created volcanic lines tracing the strike of the subducting slab. Burkart and Self [1985] made a simpler explana-

tion for the right steps in northern Central America, attributing them to upper plate structures related to the strike-slip boundary crossing Guatemala that separates the North American and Caribbean plates. The data presented below strongly support a similar upper plate origin for the right steps.

[3] Stoiber and Carr [1973] and Carr *et al.* [2003, 2007a] measured the volumes of extrusive volcanics comprising the volcanic front, including both volcanic massifs and well determined tephra volumes, expressed as dry rock equivalent volumes. Kutterolf *et al.* [2008] greatly improved the measured tephra volumes in Central America, especially the distal volumes. Table 1 has newly revised volumes of the volcanic centers in Central America using the results of Kutterolf *et al.* [2008] and Carr *et al.* [2007a]. We obtain edifice volumes by subtracting our older tephra volumes from our published volumes of volcanic centers [Carr *et al.*, 2003, 2007a]. We convert the tephra masses from Kutterolf *et al.* [2008] to km^3 using a density of 2800 kg/m^3 and add them to edifice volumes to obtain total volumes. The result, Figure 1b, is a reasonable estimate for the spatial variation in measurable extrusives. Carr *et al.* [2007a] estimated an extrusive flux based on basal ages of 600 Ka in Costa Rica and 330 Ka in Nicaragua. They implicitly assumed that the appropriate units were the extrusive mass of an entire volcanic segment and the time since the beginning of the current episode of robust activity. Kutterolf *et al.* [2008] estimate fluxes for individual centers based on the age of first eruptions of individual centers. Large variations in age lead to large variations in flux. We prefer to avoid the many assumptions needed to

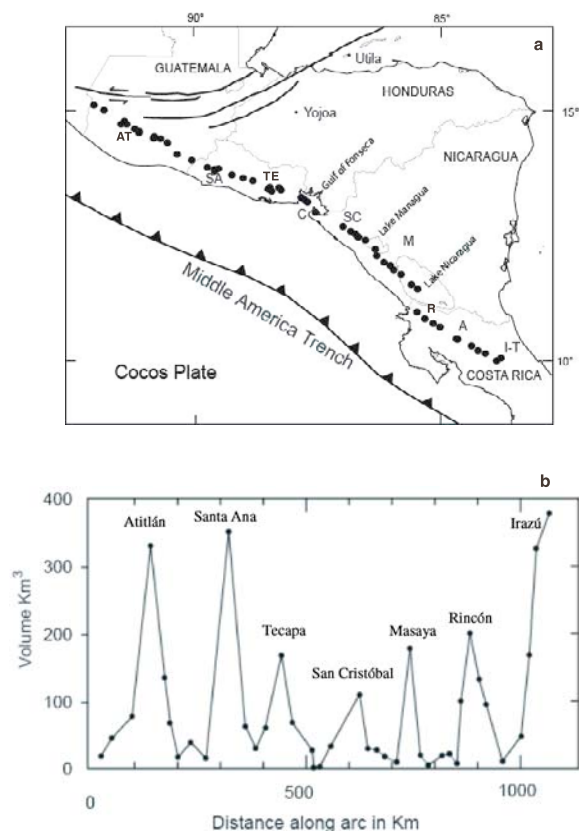


Figure 1. (a) Map of the volcanic front of Central America. The labeled volcanic centers are as follows: AT, Atitlán; SA, Santa Ana; TE, Tecapa; C, Cosigüina; SC, San Cristóbal; M, Masaya; R, Rincón de la Vieja; A, Arenal; I-T, Irazú-Turrialba. (b) Plot of eruptive volume of each volcanic center in km³ versus distance along the volcanic front in km. Left-lateral faults across central Guatemala are the Caribbean–North American plate boundary.

estimate fluxes by using a basic measurement, the actual volumes of the active volcanoes. The eruptive volumes of the centers comprising the volcanic front are highly variable (Figure 1b). In many cases, large volcanoes are flanked by progressively smaller volcanoes on each side.

[4] The well documented regional variation in slab signal along the Central American volcanic front [e.g., *Patino et al.*, 2000] is independent of both the volcanic segments and the volume distribution. The variations in trace elements are well described by Ba/La and La/Yb (or Yb/La used below). Ba/La is a proxy for fluid from the subducted slab and Yb/La is a proxy for degree of melting. Both of these ratios are highest in Nicaragua and decrease outward to Costa Rica and El Salvador (Figures 2a and 2b). The apparent positive correlation between slab signal (Figure 2a) and degree of melting

(Figure 2b) suggests that the regional variation is fundamentally a variation in degree of melting that is caused by differential delivery of slab fluid [*Carr et al.*, 2007b]. The regional variation in slab dip (Figure 2c) is consistent with the model proposed by *Carr et al.* [1990], in which a steeper dip in Nicaragua focuses the flow of slab fluid through a smaller volume that melts to a higher degree. By contrast, in the flanking regions of El Salvador and NW Costa Rica, the dip is shallower, the volume

Table 1. Volumes of Volcanic Centers in Central America^a

Volcanic Center	Edifice	Tephra	Total
Tacaná ^b	20		20
Tajumulco ^b	45		45
Santa María/Santiaguito/ Cerro Quemado ^b	25		25
Atitlán/Tolimán/ San Pedro/Caldera ^b	79	168	247
Fuego/Acatenango ^b	135		135
Agua ^b	68		68
Pacaya/Amatitlán ^b	17	61	78
Tecuamburro ^b	39		39
Moyuta ^b	15		15
Santa Ana ^b	351	13	364
Boqueron ^b	63	1	64
Ilopango ^b	1	33	34
San Vicente/Apastapaque ^b	60		60
Tecapa/Usulután/Berlin/ Tigre/Taburete ^b	168	33	201
San Miguel/Chinameca ^b	68	16	84
Conchagua ^b	27		27
Conchaguaita ^b	1		1
Meanguera ^b	3		3
Cosigüina ^c	57	9	66
San Cristóbal ^c	109		109
Telica ^c	29		29
Rota ^c	7		7
Las Pilas-Cerro Negro ^c	28		28
Momotombo ^c	17		17
Apoyeque-Nejapa ^c	18	11	29
Masaya-Las Sierras-Apoyo ^c	198	40	238
Mombacho and Granada ^c	36		36
Zapatera ^c	9		9
Concepción ^c	31	3	34
Maderas ^c	30		30
Orosi ^c	76		76
Rincón de la Vieja ^c	102		102
Miravalles ^c	62		62
Tenorio ^c	53		53
Arenal ^c	11	1	12
Platanar ^c	84	3	87
Poas ^c	97	1	98
Barba ^c	197	18	215
Irazú-Turrialba ^c	372		372

^a Edifice volumes are the published volcanic center volumes minus the tephra volumes. Tephra volumes from *Kutterolf et al.* [2008] calculated from their Tephra Magma Mass using a density of 2800 kg/m³.

^b From *Carr et al.* [2003].

^c From *Carr et al.* [2007a].

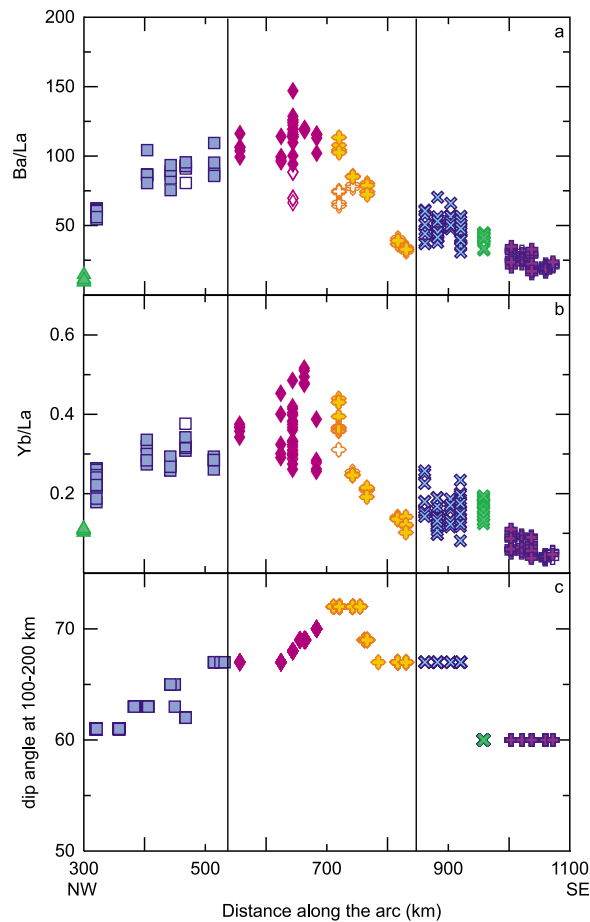


Figure 2. Regional geochemical variation along the Central American volcanic front from El Salvador through Costa Rica. The horizontal axis is distance along the volcanic front in km. Different symbols are given for each volcanic segment. El Salvador, blue squares; northern Nicaragua, pink diamonds; southern Nicaragua, orange pluses; northern Costa Rica, blue crosses; Arenal, green crosses; central Costa Rica, purple pluses. Filled symbols represent samples depleted in HFSE. Open symbols represent samples that lack strong HFSE depletion. Back-arc samples from Yojoa and Utila in Honduras (green triangles) provide a reference of asthenospheric melt with minimal to zero subducted component. (a) Ba/La, a slab signal, is maximum in Nicaragua. Ba/La does not consistently change at the right steps marked by changes in symbol type. (b) Yb/La, a proxy for degree of melting, has the same regional variation as Ba/La and also does not change consistently at the right steps separating the segments. (c) Dip of the slab between 100 and 200 km depth derived from the isobaths in the work by *Syracuse and Abers* [2006].

intersected by rising slab fluid is greater and the overall extent of melting is lower. In central Costa Rica, a subducted Galápagos component greatly changes the geochemistry [Feigenson *et al.*, 2004;

Hoernle et al., 2008] so this segment is in not readily compared to the others.

[5] Although most samples from Central American volcanoes have the typical geochemical characteristics of arc volcanism, there is a minority that has unusual characteristics, the most distinctive of which is a small depletion in high field strength elements (HFSE) or no depletion at all [e.g., *Reagan and Gill*, 1989]. We refer to these here as HFSE rich lavas because they lack the large HFSE depletions which are characteristic of arc lavas. The most extreme ones, from the Nejapa and Granada alignments in Nicaragua, were initially recognized by *Ui* [1972]. These basaltic lavas, called NG basalts by *Walker* [1984], have very low K₂O contents and TiO₂ contents between 1.0 and 2.0 wt %, rather than the low TiO₂ contents typical in arcs. Although very low K₂O contents occur primarily among the NG basalts, there is a broader distribution of basalts with TiO₂ contents greater than 1.0 wt %, compared to the 0.6 to 0.9 wt % found in the dominant group [Walker, 1984]. The distribution of basalts with >1.0 wt % TiO₂ is discontinuous. *Carr et al.* [2007b] used histograms of TiO₂ content to identify the areas where these lavas occur along the volcanic front; southeastern Guatemala [Cameron *et al.*, 2003], western and eastern Nicaragua and central Costa Rica. The eruptive volumes of these unusual magmas, estimated by *Carr et al.* [2007a], range from less than 5% in the two segments in Nicaragua to 30% in central Costa Rica. The high abundance of these lavas in central Costa Rica appears related to the incorporation of subducted Galapápagos seamounts that have an enriched OIB signature [Hoernle *et al.*, 2008].

[6] We used TiO₂ and K₂O contents to identify the scarce HFSE rich samples and included several for comparison. They are identified with open symbols in Figures 2–7. If we do not identify the HFSE rich samples using different symbols, the along strike pattern in Zr/Nb, described below, becomes less convincing in Nicaragua. However, the distinctive geochemistry of the HFSE rich lavas has been obvious since they were first described [Ui, 1972]. We agree with *Cameron et al.* [2003] that most of these lavas are decompression melts with a small subduction component. On the basis of Be and Th isotopic data, *Reagan et al.* [1994] suggest that the subduction component is substantially older. The primary trace element differences in the two magma types are shown in Figure 3. The dominant lava type is highly depleted in Nb and

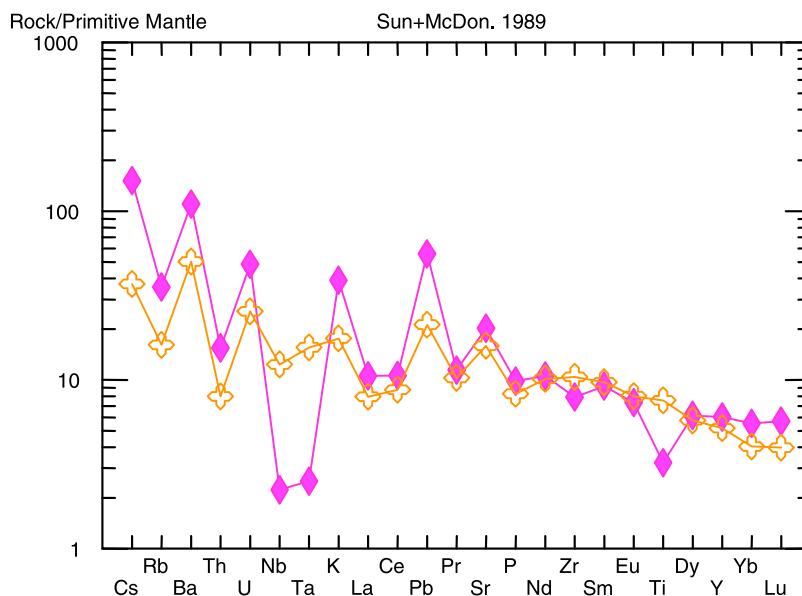


Figure 3. Spider plot with a HFSE-depleted sample, Cos5 (the filled diamonds), and a nondepleted sample, NE12 (the open pluses).

Ta, moderately depleted in Zr and Ti and enriched in Cs, Ba, U, K, Pb and Sr. The HFSE rich lava type lacks HFSE depletions and has much smaller enrichments in Cs, Ba, U, K, Pb, and Sr.

[7] Although we have systematically sought ways to link geochemical variations to the volcanic segments, no relationship has been demonstrated on a margin-wide basis. Because the relative depletion of Nb is a primary and nearly ubiquitous feature of arc volcanism it is a good candidate for revealing geochemical changes related to the right-stepping segments. Therefore, we made new trace element analyses with the goal of obtaining high-quality Nb and Ta data. The primary result is that Zr/Nb emerged as the first geochemical signature that clearly reflects the segmentation of the Central American volcanic front. In this paper we focus on the volcanic front from El Salvador through Costa Rica, which consists of the five segments we have extensively sampled. We show that Zr/Nb, a proxy for the extent of the Nb depletion, reflects the segmentation. We propose a model of melt generation and release that links the variation in Nb depletion to both segmentation and the volumes of the volcanoes.

2. Data Collection

[8] Our collection of Central American samples began in 1970. Until 1990, powders were prepared using either alumina or tungsten carbide vessels. Because the older samples powdered in tungsten

carbide were improperly prepared for Nb and Ta, we made new powders, using only alumina vessels. We then used established HR-ICP-MS techniques to upgrade the Central American data set. The samples reported in this study were chosen to be representative of the mafic component of the Central American volcanic front. Samples with SiO₂ between 45 and 60 wt % were chosen in an attempt to reduce the effects of shallow fractionation and assimilation. The new analyses are a mix of samples that had never been analyzed for trace elements by ICP-MS and samples that were already well characterized, except for Nb and Ta.

[9] All samples were analyzed for major and trace element compositions (auxiliary material).¹ Major element data were obtained by different methods, but primarily by DCP-AES (direct current plasma atomic emissions spectrometer) or XRF (X-ray fluorescence). DCP-AES analyses were performed in the Department of Geological Sciences at Rutgers University. XRF analyses were made by the Department of Geological Sciences at Michigan State University. DCP-AES analyses report FeO total, while XRF analyses report Fe₂O₃ total. The reader is referred to *Feigenson and Carr* [1985] for methods used for the DCP-AES analyses. For XRF methods, the reader is referred to *Vogel et al.* [2006].

¹Auxiliary material data sets are available at <ftp://ftp.agu.org/apend/gc/2009gc002704>. Other auxiliary materials are in the HTML.

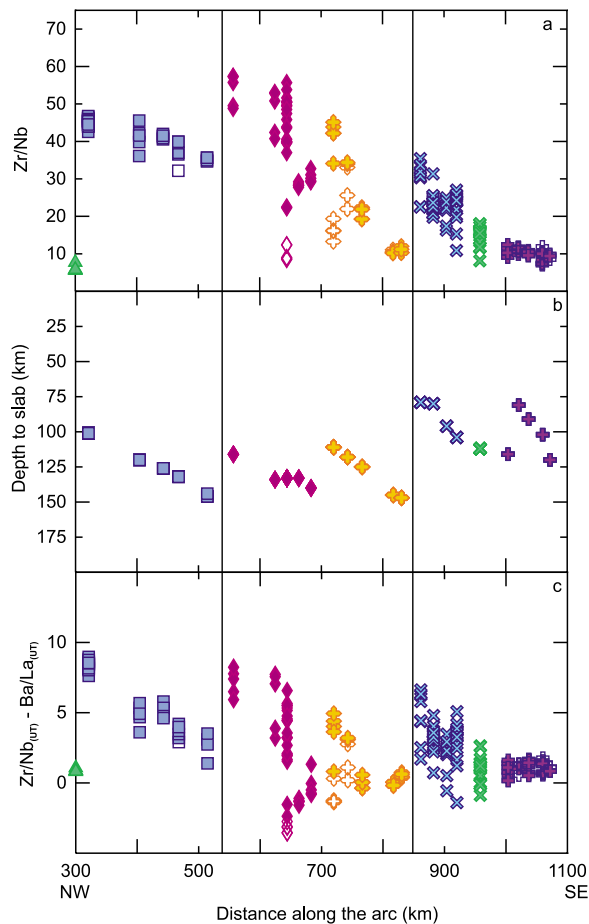


Figure 4. Sawtooth patterns in geochemical and geophysical parameters along the Central American volcanic front. The horizontal axis is distance along the volcanic front in km. (a) Zr/Nb defines a sawtooth pattern that corresponds with right steps separating the volcanic segments. (b) Slab depth in km shows the same sawtooth pattern. Slab depths are taken from *Syracuse and Abers* [2006]. (c) $Zr/Nb - Ba/La$ both normalized to the back-arc sample Utila to remove the region variation from Zr/Nb . Symbols are the same as Figure 2.

[10] Trace element analyses were performed on a Finnigan MAT High Resolution Inductively Coupled Plasma Mass Spectrometer (HR-ICP-MS) at the Institute of Marine and Coastal Sciences at Rutgers University. The back-arc Yojoa and Utila samples were analyzed at a later date on a VG PQ Excel Quadrupole Inductively Coupled Plasma Mass Spectrometer at the Department of Earth Sciences at Boston University. The same analytical techniques were used for both sample sets. The only differences between the two analytical procedures are a few interference corrections that were performed on the quadrupole ICPMS data. Unlike

the HR-ICPMS, the quadrupole cannot resolve isobaric interferences.

[11] Samples prepared for trace element analyses were digested using a HF/8 N HNO_3 mixture, followed by additional fluxes of 8 N HNO_3 . For more detailed methods, the reader is referred to *Bolge et al.* [2006] or *Bolge* [2005]. Along with each batch of 12–15 samples a digestion blank and a USGS rock standard, either BHVO-1 or AGV-1, was also digested to check any possible contamination as well as the precision and accuracy of the digestion process. These USGS standards were selected because these encompass the chemical range of the samples. Standard addition curves consisted of four points and had R^2 values of 0.999 or better. Average slopes of the standard curves were used to calculate concentrations. An average digestion blank for each run was also calculated and subtracted from all the samples. The digestion blanks were generally low and constant from blank to blank. Replicate digests of samples and USGS standards measured the precision of the entire digestion/preparation process. The USGS standards were also used to measure the accuracy of the analyses. Since there is no clear consensus on which preferred values are used for many of the trace elements, different labs tend to use their own accepted values for these rock stand-

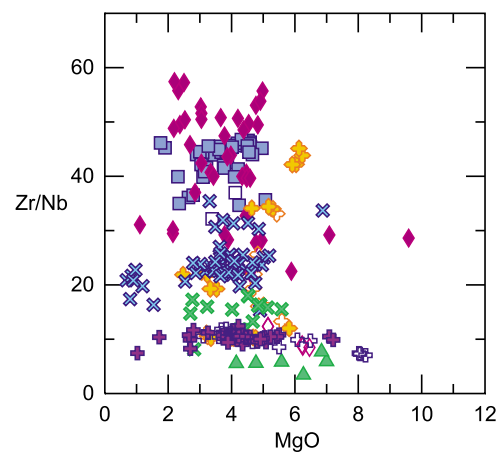


Figure 5. MgO versus Zr/Nb . Central Costa Rican samples have a narrow range between 7 and 10, whereas other segments of the margin have substantially larger ranges. The central Costa Rican samples have similar values consistent with a Galápagos component with minor subsequent Nb depletions. The rest of Central America has a Zr/Nb range of 10 to 60 which could result from mixing of a MORB component, a Galápagos component, and an additional component with elevated Zr/Nb most likely from subduction derived fluids. Symbols are the same as Figure 2.

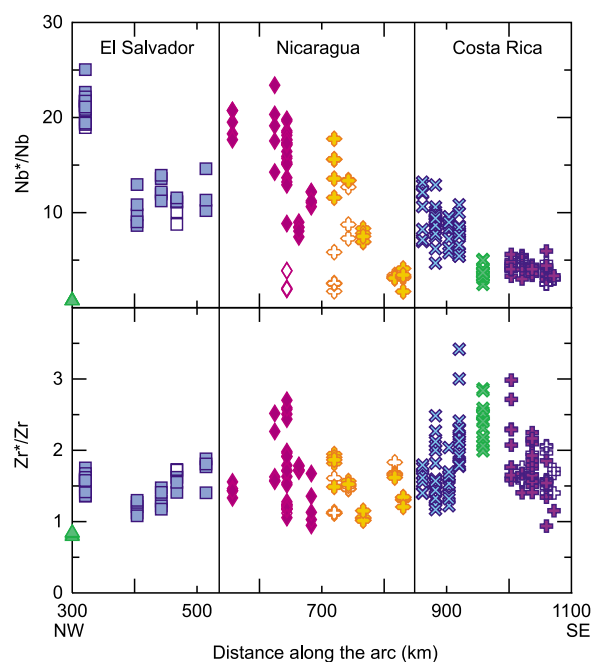


Figure 6. HFSE depletions versus distance along the volcanic front. Nb^* is estimated using the values of U and K and primitive mantle normalization factors $U = 0.21$ ppm, $K = 250$ ppm, and $Nb = 0.73$ ppm [Sun and McDonough, 1989]. Zr^* is estimated using the values of Nd and Sm and primitive mantle normalization factors $Nd = 7.3$ ppm, $Sm = 2.63$ ppm, and $Zr = 74$ ppm [Sun and McDonough, 1989]. Nb depletions are much greater than Zr depletions. The three sharp increases in Nb^*/Nb , in NW Nicaragua, central Nicaragua, and NW Costa Rica, correspond to the increases seen in Zr/Nb . In combination these plots indicate that the sawtooth pattern in Zr/Nb is primarily caused by changing Nb depletion. Symbols are the same as Figure 2.

ards. By using synthetic multielement standards rather than USGS rock standards to standardize, the USGS rock concentrations we measured can be used by others to normalize this data set to whatever their individual preferred values are. The measured values for these USGS rock standards along with their precision and the average blanks are listed in the auxiliary material. For all geochemical plots the error bars on each element or elemental ratio is smaller than the symbol size.

3. Results

3.1. Segmented Regional Geochemical Variation of Zr/Nb

[12] Zr/Nb defines five distinct segments from central Costa Rica northwestward through El Salvador (filled symbols in Figure 4a). The unusual

lavas that lack the typical HFSE depletion (open symbols) do not show the segmented pattern. The sawtooth pattern defined by Zr/Nb is similar to the distribution of depths to the seismic zone (Figure 4b) published by Syracuse and Abers [2006]. In central Costa Rica, Zr/Nb is constant and at a typical OIB value (10 ± 3); in NW Costa Rica, SE Nicaragua, NW Nicaragua and El Salvador, there are gradual northwestward increases in Zr/Nb separated by large and abrupt drops. Abrupt drops occur at each of the segment boundaries noted by Stoiber and Carr [1973]. The break between central Costa Rica and northern Costa Rica was proposed by Liaw and Matumoto [1980] on the basis of an apparent offset in seismicity near Arenal volcano. However, Protti et al. [1995] did not find an offset there. Arenal, a young (less than 100 Ka) volcanic complex, occurs in the center of what is otherwise the widest volcanic gap in Central America but there is no offset or change in strike of the volcanic line. Arenal is a geochemical intermediate between NW Costa Rica and central Costa Rica and therefore is not grouped with either segment. Similarly, there is no offset in Zr/Nb at this break. The Zr/Nb sawtooth and the sawtooth pattern of depths to the seismic zone are similar in having offsets at the same places and by systematically varying within each segment. They differ in scale and the overall regional shape differs, and so there is no linear correlation between Zr/Nb and depth.

[13] All of the segment boundaries with large offsets in Zr/Nb also have right steps in the volcanic front (Figure 1a). Above the smoothly varying subducted slab, the abrupt right steps in the volcanic front result in abrupt increases in depth to the slab on the NW side. The corresponding large decreases in Zr/Nb indicate a reduction in the degree of Nb depletion with depth to the subducted slab. Similarly, the gradual decreases in Zr/Nb to the SE within a segment correlate with increasing depths to the slab and corresponding decreases in Nb depletion.

[14] For the margin as a whole, there is no correlation between depth to the slab and Zr/Nb because there is margin-wide regional variation in Zr/Nb with the highest values in Nicaragua. This regional variation is similar to those noted by Patino et al. [2000] for slab fluid tracers, such as Ba/La (Figure 2a) and U/Th. Although Zr/Nb has an overall positive correlation with these slab tracers, the correlation arises from intersegment variation. Within an individual segment, there is no correlation between

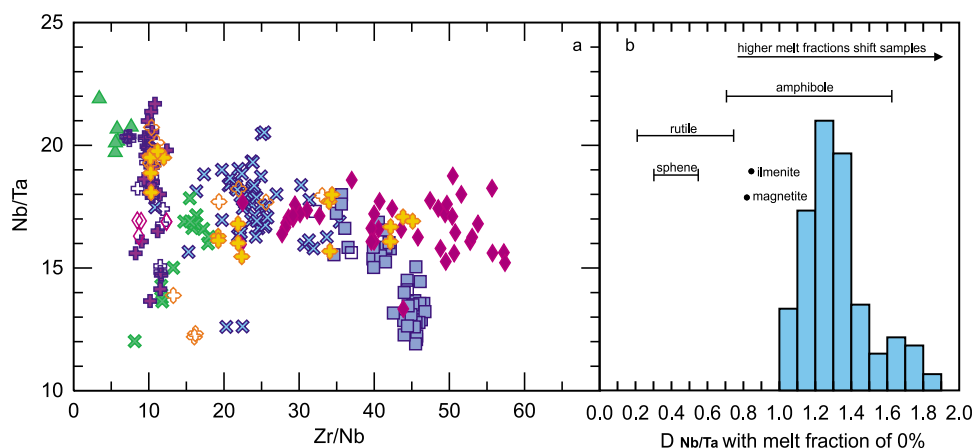


Figure 7. Nb/Ta and identification of HFSE retaining mineral. (a) Zr/Nb versus Nb/Ta. From Nicaragua to NW Costa Rica, there is substantial variation in Zr/Nb but not in Nb/Ta with most ratios between 15 and 19. NW Costa Rica and SE Nicaragua have samples that span the range covered by central Costa Rica, suggesting that at least some of the subducted seamount component is reaching these areas. Over a large range of Nb depletion, Nb/Ta essentially maintains a mantle value. In contrast, there is a negative correlation between Zr/Nb and Nb/Ta in El Salvador. (b) Histogram of estimated D_{Nb}/D_{Ta} using the back-arc sample, Utila, as the mantle composition. Experimental ranges of D_{Nb}/D_{Ta} for possible Nb retaining minerals are from *Green and Pearson* [1987], *Klemme et al.* [2005], and *Tiepolo et al.* [2002, 2000]. Major minerals, such as olivine, orthopyroxene, clinopyroxene, and garnet, were not included in this plot because these minerals do not contain large enough amounts of Nb or Ta to cause the depletions.

Zr/Nb and Ba/La, Yb/La or U/Th but there are moderate negative correlations between slab depth and Zr/Nb within the segments.

[15] We sought a geochemical method to subtract Ba/La from Zr/Nb and thereby remove the regional variation. Because these ratios have very different means and ranges we recast all four elements as multiples of a lava from Utila Island (Figure 1a) that appears completely free of slab contribution. This island is off the north coast of Honduras and near the strike-slip boundary between the North American and Caribbean plates. $Ba/La_{(UT)}$ is $(Ba/Ba_{(utila)})/(La/La_{(utila)})$. This works out to be Ba/La divided by 12.3. Similarly, $Zr/Nb_{(UT)}$ is Zr/Nb divided by 3.4. The difference, $Zr/Nb_{(UT)} - Ba/La_{(UT)}$ in Figure 4c, is an attempt to see just the depth-dependent variation in Zr/Nb. This manipulation removes much but not all of the regional variation, resulting in an along strike variation that is somewhat closer to the variation in depths to the seismic zone. This attempt does demonstrate that Zr/Nb is not a simple function of depth to the seismic zone.

3.2. High Field Strength Element Correlations

[16] Zr and Nb are relatively insoluble in aqueous liquids [Woodhead et al., 1993] but incompatible

during melting of common mantle minerals. HFSE in arc magmas are commonly depleted relative to other elements with similar incompatibilities, but such depletions are not seen in MORB or OIB magmas. Depletions in $HFSE^{+5}$ (Nb, Ta) are generally more pronounced than depletions in $HFSE^{+4}$ (Zr, Hf, Mo and W). In Central America there is high correlation between HFSE with the same valence, especially Nb versus Ta and Zr versus Hf. However, two distinctive distributions of $HFSE^{+5}$ versus $HFSE^{+4}$ (e.g., Zr/Nb) occur: central Costa Rican samples plot near Zr/Nb = 10 with a narrow range between 7 and 10, whereas other segments of the margin have substantially larger ranges. El Salvador (squares in Figure 5) has the second narrowest range for 32 to 47. The low and near constant Zr/Nb in central Costa Rica suggests a different process or source. Galápagos hot spot volcanics have Zr/Nb ratios of approximately 4 to 9 [Kamber and Collerson, 2000]. The central Costa Rican samples have similar values consistent with a Galápagos component with minor subsequent Nb depletions. The Pb isotopic characteristics of these volcanoes strongly argue for a Galápagos component in the source [Feigenson et al., 2004; Hoernle et al., 2008]. The rest of Central America has a Zr/Nb range of 10 to 60 which could result from mixing of a MORB component and a Galápagos component. However, some of the Zr/Nb



compositions are well above both of these compositions, therefore an additional component with elevated Zr/Nb must be present. This component must come from subduction derived fluids.

[17] Lower Zr/Nb values are also present in the unusual HFSE rich samples from Nicaragua. *Klemme et al.* [2002, and references therein] showed that Ti solubility is substantially higher at higher temperatures and pressures leading to an elimination of negative HFSE anomalies. The HFSE-rich samples from Nicaragua may result from magma coming from a deeper hotter region of the mantle. Most of central Costa Rican samples have a small Nb depletion and so the high-temperature explanation cannot explain these small but real depletions.

[18] Both Zr and Nb are depleted in the typical volcanic front samples (e.g., Figure 3, diamonds). We estimated depletions of Nb and Zr using Nb*/Nb and Zr*/Zr (Figure 6). Nb depletions are much greater than Zr depletions. The three sharp increases in Nb*/Nb, in NW Nicaragua, central Nicaragua and NW Costa Rica correspond to the increases seen in Zr/Nb. Comparison of the Nb*/Nb and Zr*/Zr plots in Figure 6 indicates that the sawtooth pattern in Zr/Nb is primarily caused by changes in Nb depletion.

4. Discussion

4.1. What Mineral Is Controlling the HFSE Depletions?

[19] There are two explanations for the HFSE depletions in arc magmas: (1) a mineral/fluid partitioning process in the mantle wedge sequesters the HFSE and (2) fluid or melt from the subducting slab preferentially adds to the wedge all incompatible elements except HFSE which are retained in the subducting crust. A major difference between the two theories is the location of the HFSE depletion event; in the subducted crust as it releases an incompatible element-rich but HFSE-poor fluid, or in the mantle wedge as a melt forms and then rises to the surface. For both theories, one or more minerals are responsible for holding onto the HFSE. Some possible HFSE retaining minerals are Ti bearing oxides such as rutile, sphene, magnetite and ilmenite or Ti-rich amphiboles and micas.

[20] The HFSE ratios Zr/Nb and Nb/Ta behave very differently (Figure 7a) and there is no correlation between them except in El Salvador (filled

squares in Figure 7a). For most of the margin there is wide variation in Zr/Nb and limited variation in Nb/Ta, which has a mean of 17.1, very close to the nominal mantle value [*Green, 1995*]. Samples from central Costa Rica (purple pluses in Figure 7a) have a very different distribution, with limited variation in Zr/Nb and a wide range in Nb/Ta from 13.5 to 22. Because this area has a subduction derived Galápagos component and since the Galápagos islands have a substantial range in Nb/Ta, from at least 9.5 to 18 [*Geist et al., 2006; Kurz and Geist, 1999*], we attribute much of this range to the input of subducted Galápagos seamounts. The upper end of the range is similar to the Nb/Ta ratios found at Utila and Yojoa in Honduras (Figure 1a), suggesting a mantle contribution as well. These alkaline basalts presumably sample the continental lithosphere or the enriched veins in the mantle inferred by *Feigenson and Carr* [1993] from REE data. An additional complication in central Costa Rica is that Sr/Y reaches 55 and more than half the samples have Sr/Y ratios greater than 30, implying that the subducted seamount contribution is a melt with residual garnet and not a fluid. These samples have the same positive correlation between Zr/Sm and Nb/La and negative correlation of Zr/Sm and Nb/Ta that *Münker et al.* [2004] found for samples in the western Aleutians and north-central Kamchatka that are considered derived from slab melts. These systematics indicate variable proportions of amphibole and rutile in the sources of the slab melts [*Münker et al., 2004*].

[21] From Nicaragua to NW Costa Rica, there is substantial variation in Zr/Nb but a limited dispersion of Nb/Ta, with most ratios between 15 and 19. NW Costa Rica and SE Nicaragua have samples that span the range covered by central Costa Rica, suggesting that at least some of the subducted seamount component is reaching these areas [*Hoernle et al., 2008*]. It is surprising that over a large range of Nb depletion, Nb/Ta essentially maintains a mantle value. In contrast, there is a negative correlation between Zr/Nb and Nb/Ta El Salvador (blue squares in Figure 7a). *Abers et al.* [2003] provides seismic evidence that there is an unusually wet slab beneath Nicaragua. *Eiler et al.* [2005] found low oxygen isotopes in Nicaragua, consistent with fluids derived from serpentine. It is not clear that greater amounts of fluid would directly change the Nb/Ta ratio but different fluid fluxes could change the temperatures, pressures and mineral stabilities controlling fluid release from the slab and wedge melting between El Salvador and Nicaragua.



[22] The negative correlation of Nb/Ta and Zr/Nb in El Salvador suggests that a mineral retains Nb and Ta differentially; with increasing retention of Nb, Nb/Ta decreases, implying $D_{\text{Nb}}/D_{\text{Ta}} > 1.0$. In Figure 7b we estimate the residue's $D_{\text{Nb}}/D_{\text{Ta}}$ for each sample by assuming batch melting, a melt proportion (F) and a source composition. At $F = 0$, the batch melting equation $C_{\text{melt}} = C_{\text{residual}}/(F + D(1 - F))$, simplifies to $C_{\text{melt}} = C_{\text{residual}}/D$ and $D_{\text{Nb}}/D_{\text{Ta}}$ becomes $(\text{Nb}/\text{Ta})_{\text{mantle}}$ times $(\text{Ta}/\text{Nb})_{\text{melt}}$. The back-arc lava, UT1, was used to represent the mantle composition with Nb/Ta of 22. This ratio is appropriate for the subcontinental lithosphere of Honduras but may be too high for the volcanic front samples. Using a Nb/Ta value of 22 for the mantle, most estimated $D_{\text{Nb}}/D_{\text{Ta}}$ ratios are between 1.0 and 1.8 (Figure 7b). Using the nominal mantle Nb/Ta value of 17.5 shifts the histogram left to a range between 0.8 and 1.6. If a realistic F of 15% is used, the histogram is shifted back toward higher values. The mineral or combination of minerals retaining Nb and Ta needs to have a $D_{\text{Nb}}/D_{\text{Ta}}$ of 1.0 or higher. For partitioning between minerals and silicate liquid, only amphibole has a $D_{\text{Nb}}/D_{\text{Ta}}$ greater than 1, therefore amphibole is likely the dominant mineral controlling the Nb depletions in Central America. Other minerals such as rutile may also be present and contributing to the depletions. Varying combinations of any of the minerals can produce the calculated $D_{\text{Nb}}/D_{\text{Ta}}$ values as long as amphibole is also included to provide a high $D_{\text{Nb}}/D_{\text{Ta}}$ values.

[23] *Brenan et al.* [1994] measured rutile/aqueous fluid partition coefficients. Their results for $D_{\text{Nb}}/D_{\text{Ta}}$ (0.83–1.57) are essentially that same range as amphibole in a melt. Therefore, the Central American data could be a result of a fluid interacting with rutile rather than a melt interacting with amphibole. The problem then shifts to constraining this fluid and determining whether or not it will explain the Central America data. *Becker et al.* [1999] examined high-pressure veins found in eclogites from paleosubduction zones. The low amount of volatiles in these veins indicate some loss before precipitation, but the veins put some limits on the fluid [*Becker et al.*, 1999]. Compared with eclogite, the veins are enriched in Cs, Rb, K, Ba, and Pb, unchanged in U, Th, Sr, and depleted in Nd, Sm, Y, Ti, Nb, and Zr relative to MORB [*Becker et al.*, 1999]. The lack of enrichment in U, Th, and Sr indicate an aqueous fluid rather than a melt [*Becker et al.*, 1999]. *Becker et al.* [2000] compared eclogite to altered oceanic basalt to

determine the fluid composition. The eclogite had large depletions in K, Ba and Rb compared to the equally incompatible Nb, U, Th. *Becker et al.* [2000] attributed this to the selective removal and breakdown of K-bearing hydrous phases during dehydration. The dehydration showed little to no loss for HFSE, Th, Sr, Nd, Sm, Y, Cr, Co, and Ni [*Becker et al.*, 2000].

[24] The eclogites examined by *Becker et al.* [1999, 2000] showed retention not only of the HFSE, but also other elements (U, Th, Sr and HREE) that are not depleted in Central American lavas. Because the Central American lavas have enrichments in U, Sr and, to a lesser extent, Th and no depletions of the HREE, the HFSE depletions are more likely the result of retention by mineral/melt reactions than by mineral/aqueous fluid reactions. This argument favors amphibole as the Nb retaining phase.

4.2. Pressure-Dependent Mineral Reaction

[25] Because Zr/Nb and slab depth change sympathetically, there may be a mineralogical change with depth that controls Zr/Nb. Our observation is that within each segment, as slab depth increases, Nb increases in the melt, lowering the Zr/Nb ratio. If Nb increases in the melt, it decreases in the residue as the mineral retaining Nb breaks down with increasing pressure. Unlike rutile which becomes more stable with increasing pressure, amphibole becomes unstable [*Xiong et al.*, 2005]. The pargasite amphibole stability in a MORB composition is approximately 30 GPa [*Niida and Green*, 1999] and the breakdown of amphibole occurs over a range of pressures. *Foley* [1991] found that the upper pressure limit of pargasitic amphibole could be elevated an additional 15 GPa, if the pargasite tends to the fluor rather than the hydroxyl end-member. This puts pargasitic amphibole in the same depth range as the slab depths in Central America. *Niida and Green* [1999] found that the Ti-tschermakite component of amphibole decreases slightly with increasing pressure. These experimental results are consistent with our inference of decreasing Nb retention with depth. Therefore, amphibole fits our observation requiring a pressure-dependent Nb retaining mineral. The variable release of Nb from amphibole can be a complex function of slab dip, depth, temperature and composition and plausibly fits our observation that Nb depletion decreases with depth to the slab locally (within a segment) but does not define a

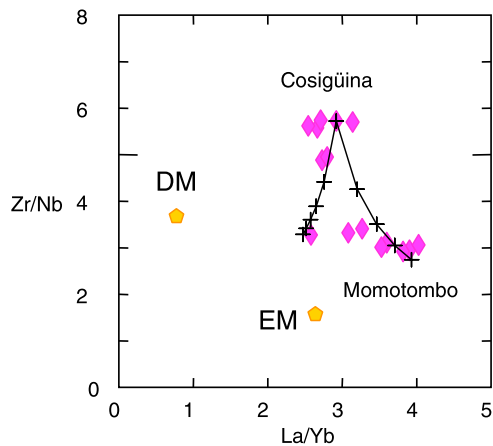


Figure 8. AFC model that derives the range of Momotombo data from a representative sample from Cosigüina (Cos-HH). The upper seven points are from Cosigüina, and the rest are from Momotombo. The model on the right-hand side is obtained by assimilating EM, using AFC modeling ($r = 1.05$, $F = 100\% - 120\%$, and $\text{step} = 5\%$), a mantle mode of $60\text{ol} + 20\text{opx} + 20\text{cpx}$, and partition coefficients from *Kelemen et al.* [2003]. Model of the left-hand side differs by assimilating DM with $F = 100\% - 200\%$ and $\text{step} = 20\%$.

margin-wide correlation between Nb depletion and depth to the slab.

4.3. Zr/Nb Controlled by Flow Through the Mantle Wedge

[26] In the previous model, more Nb is added from the subducting slab to the mantle wedge with increasing depth. Another possibility is that the amount of Nb coming off the slab is constant, regardless of slab depth. In this model, all melts begin with large Nb depletions and Nb is added to the melt as it rises through and reacts with the mantle wedge. The longer the melt path becomes, the more interaction/assimilation with the mantle wedge Nb and the lower the Nb depletion. This can be modeled using AFC equations [DePaolo, 1981] and appropriate partition coefficients [Kelemen et al., 2003]. In Figure 8, we plot the data for the two volcanoes in western Nicaragua that span the extremes in Zr/Nb for that segment. Cosigüina, with high Zr/Nb has a much shallower depth to the slab than Momotombo on the other end of this segment. We assume that the melt from Cosigüina travels a short distance through the mantle wedge and its Zr/Nb is unchanged from the ratio of the initial melt. Momotombo magma has a longer path through the wedge and thus reacts with more mantle. Starting with a representative Cosigüina sample, the Momotombo samples are bracketed by

AFC models that use DM and EM mantle as assimilants. We use the EM and DM from *Feigenson et al.* [1996] and set $r = 1.05$. The r is the mass of magma/original mass or Mm/Mo. With $r = 1.05$ we assume that the rising fluid is increasing in mass which may well occur for melts interacting with mantle. Although plausible fits (Figure 8) can be obtained through a melt reaction model, there is a basic difficulty; there is not a good correlation between depth to the slab and Zr/Nb which would be expected from this simple model.

4.4. Tectonic Implications and Speculations

[27] The regional variations in Zr/Nb and depth to the seismic zone (Figure 4) require the smooth slab mapped by *Syracuse and Abers* [2006] rather than the segmented slab proposed by *Stoiber and Carr* [1973]. The narrow volcanic front cuts across the isobaths to the seismic zone providing a range of depths to the zone. Because small volcanoes are typically near offsets in the volcanic front and large ones are typically within segment interiors, the distribution of extrusive volcanic output appears to be linked to the crosscutting strike of the volcanic front segments. In Figure 9, we define an axis of volcanic productivity by connecting the largest volcanoes by a line that does not intersect the smaller volcanoes. We also assume that volcanoes with very low Zr/Nb are behind the axis of productivity and those with very high Zr/Nb are in front of the axis of productivity. The volcanic

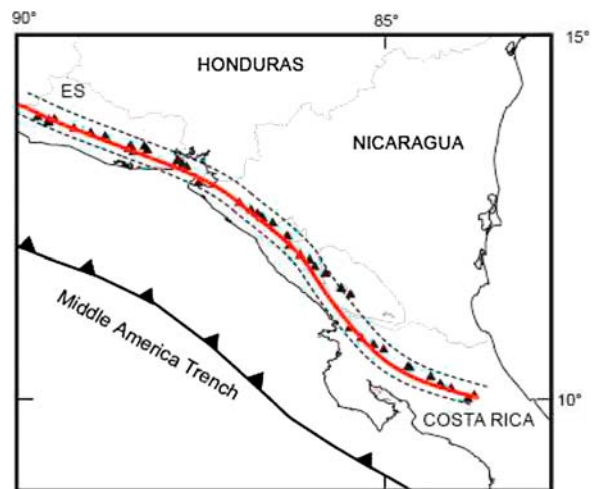


Figure 9. Volcanic productivity axis. The solid red line is defined by connecting all the largest volcanoes, the ones named in Figure 1b. This productivity axis is then bracketed by drawing parallel lines that encompass all vents and define a zone of eruptive potential.

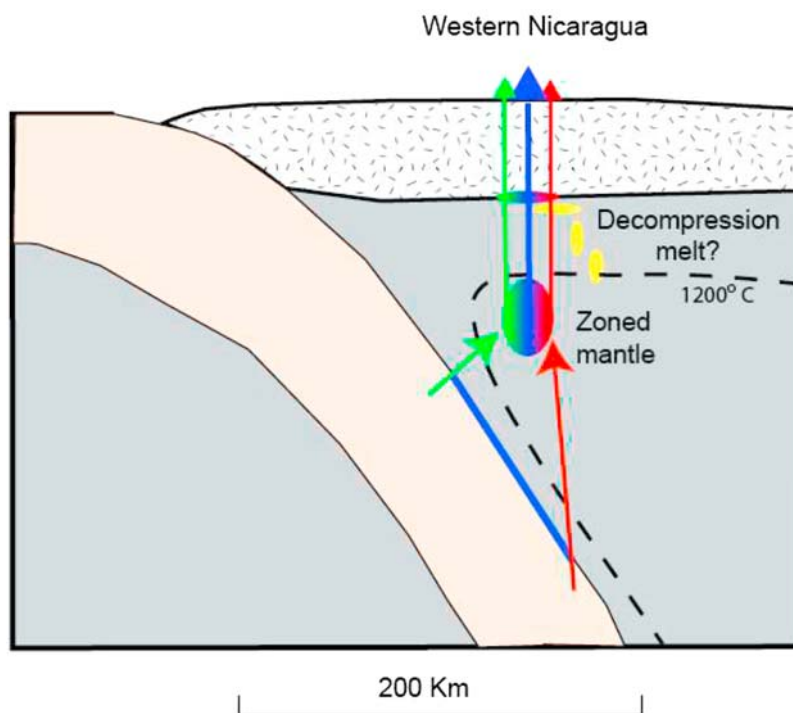


Figure 10. Intrasegment variations in Zr/Nb and volcano size. A cross section of western Nicaragua with volcanoes is projected along strike onto the mantle structure. The largest volcano (blue) is San Cristóbal, which sits above the center of the melt zone. Smaller volcanoes are off the productivity axis and tap less of the melt. Cosigüina (green) has a short path through the mantle wedge and rises from the shallowest part of the descending slab, where Nb retention is at a minimum. The opposite is Momotombo, a long path, a deep slab, and minimum Nb depletion. Scaled to *Syracuse and Abers's* [2006] map. Decompression melting moving in from back arc is not ruled out.

centers we connect are the ones named in Figure 1b. We define a zone of eruptive potential by drawing parallel lines that bracket the axis and encompass all the vents. This zone may well map the surface extent of the melt aggregation zone in the mantle wedge. The variations in Zr/Nb and volume result from the difference in strike between the volcanic front and the subducting slab. In cross section (Figure 10) we show a mantle wedge structure that is perpendicular to the subducting slab and so identical all along the segment. We project volcanoes from the middle and both ends of the segment onto the cross section. The volcano at the northwest end of the segment is above the shallowest part of the slab and has maximum Zr/Nb. It is a small volcano because it sits on the trenchward margin of the zone of eruptive potential and is relatively starved for magma input, receiving only magma with high Nb depletion. The volcano in the center of the segment has moderate Zr/Nb and the largest volume. It draws magma from the entire zone, thus it is large and has an average Nb depletion. The volcano at the southeast end of the segment is above the deepest part of the slab and has minimum Zr/Nb. It is a small volcano because

it sits on the landward margin of the zone of eruptive potential and is relatively starved for magma input, receiving only magma with minimal Nb depletion. This simple model requires the volcanic front to be an upper plate structure.

[28] *Stoiber and Carr* [1973] pointed out that there were no obvious faults connecting the aligned volcanic centers in a single segment. In fact, the surface structures most closely parallel to the volcanic lines are right-lateral strike-slip faults located either in front of or behind the volcanic lines. They therefore proposed that the volcanic segments were parallel to the strike of the underlying seismic zone. This assumption is now proven wrong but the question of the origin of the offset and crosscutting volcanic front lineaments remains. In global plate models, the Cocos-Caribbean convergence has been poorly constrained. Early plate circuits used the P axes of focal mechanisms along the Middle America Trench, which resulted in margin perpendicular convergence [e.g., *Chase*, 1972; *Molnar and Sykes*, 1969]. GPS campaigns have now defined a more oblique convergence vector for this margin [e.g., *DeMets*, 2001] giving



rise to fore-arc slivers migrating NW relative to the Caribbean plate [Lundgren *et al.*, 1999]. This is the likely explanation of the margin parallel right-lateral strike-slip faults. Another feature of the structure of Central America is the common presence of N-S extensional structures like the Managua graben in Nicaragua [Girard and van Wyk de Vries, 2005], the Gulf of Fonseca and the Guatemala City graben [Stoiber and Carr, 1973]. N-S vent alignments are common along the volcanic front but large transverse extensional structures occur only at the right steps between the volcanic lines. We speculate that the volcanic front is a series of leaky right-lateral faults, connected by N-S striking rifts at the segment boundaries where the volcanic front steps to the right.

[29] The segmented structure remains to be explained. Geochronological work, summarized by Carr *et al.* [2007a] indicates that the present volcanic front in Nicaragua and Costa Rica took its present location about 2 to 4 Ma ago. Prior to that, the volcanic front in Nicaragua and northern Costa Rica, was substantially further inland and had its last major activity about 7 Ma ago. Rogers *et al.* [2002] propose a slab tear off sometime after 10 Ma ago to explain the subsequent large uplift across much of Honduras. For our purposes, we will assume that a reorganization of plate subduction took place at 7 Ma. Between 7 Ma and the resumption of robust volcanism at about 2 Ma in northern Costa Rica and Nicaragua, there was a prolonged pause in robust volcanism [Saginor *et al.*, 2009]. In Nicaragua, the new volcanic front rose 30 km seaward of the former front. This pause and jump of the volcanic front suggests that magma rose to a new position beneath the crust/lithosphere. It did not erupt immediately but instead heated and weakened the upper plate. The location of the weakening became the zone of eruptive potential (dashed lined enclosed region in Figure 9). Oblique convergence stressed the Caribbean plate which ruptured in right-lateral tears crossing the weakened zone in an echelon fashion. These tears became the volcanic front lineaments. We speculate that the tearing began at the base of the crust/lithosphere with magma rising vertically.

5. Conclusions

[30] Because of the segmented structure of the volcanic front, the depth to the slab defines a sawtooth pattern. Proceeding northwest there are sharp increases in depth to slab at the beginning of

each volcanic segment whereas within each segment, slab depth shallows to the NW. This pattern is the result of upper plate structures that create a series of right-stepping volcanic lines or segments that strike slightly counterclockwise to the strike of the slab.

[31] Zr/Nb is the first geochemical signature with consistent large offsets at the right steps in the volcanic front. Moreover, Zr/Nb mirrors the sawtooth variation in depth to the slab. Within a segment it increases from SE to NW and at the right steps, separating segments, it abruptly decreases. There is no simple negative correlation between Zr/Nb and depth to the slab because Zr/Nb also has a regional variation, similar to previously documented regional variations in slab tracers in Central America (e.g., Ba/La, U/Th, $^{87}\text{Sr}/^{86}\text{Sr}$). Estimates of Nb and Zr depletion (Nb^*/Nb and Zr^*/Zr) indicate that the Zr/Nb signal is primarily one of Nb depletion.

[32] The decrease in Nb depletion with depth to slab can be explained in one of two ways. First, a Nb retaining mineral in the subducting slab is breaking down with increasing depth thus releasing more Nb into the overlying mantle wedge and causing smaller Nb depletions with depth. In El Salvador, the negative correlation between Zr/Nb and Nb/Ta argues that amphibole is the dominant Nb-retaining mineral. In other segments, amphibole is needed but rutile or other minerals with $D_{\text{Nb}}/D_{\text{Ta}} < 1$ can be involved. Second, all melts start with the same Nb depletion but as they rise through the mantle wedge they react with the surrounding mantle and gain Nb. Consequently, a deeper melt with a longer path will react more with the mantle wedge causing a greater dilution/reduction of the initial Nb depletion.

Acknowledgments

[33] We would like to thank the countless friends, students, and scientists that helped collect the Central American volcanic rock samples over the past 40 years. This study received partial support from NSF grants EAR-0507924 and EAR-0203388.

References

- Abers, G. A., T. Plank, and B. R. Hacker (2003), The wet Nicaraguan slab, *Geophys. Res. Lett.*, *30*(2), 1098, doi:10.1029/2002GL015649.
- Becker, H., K. P. Jochum, and R. W. Carlson (1999), Constraints from high-pressure veins in eclogites on the composition of hydrous fluids in subduction zones, *Chem. Geol.*, *160*, 291–308, doi:10.1016/S0009-2541(99)00104-7.



- Becker, H., K. P. Jochum, and R. W. Carlson (2000), Trace element fractionation during dehydration of eclogites from high-pressure terranes and the implications for element fluxes in subduction zones, *Chem. Geol.*, *163*, 65–99, doi:10.1016/S0009-2541(99)00071-6.
- Bolge, L. L. (2005), Constraining the magmatic sources of Hawaiian and Central American volcanics, Ph.D. thesis, Rutgers Univ., New Brunswick, N. J.
- Bolge, L. L., M. J. Carr, M. D. Feigenson, and G. E. Alvarado (2006), Geochemical stratigraphy and magmatic evolution at Arenal Volcano, Costa Rica, *J. Volcanol. Geotherm. Res.*, *157*, 34–48, doi:10.1016/j.jvolgeores.2006.03.036.
- Brenan, J. M., H. F. Shaw, D. L. Phinney, and F. J. Ryerson (1994), Rutile-aqueous fluid partitioning of Nb, Ta, Hf, Zr, U and Th: Implications for high field strength element depletions in island-arc basalts, *Earth Planet. Sci. Lett.*, *128*, 327–339, doi:10.1016/0012-821X(94)90154-6.
- Burkart, B., and S. Self (1985), Extension and rotation of crustal blocks in northern Central America and effect on the volcanic arc, *Geology*, *13*, 22–26, doi:10.1130/0091-7613(1985)13<22:EAROCB>2.0.CO;2.
- Cameron, B. I., J. A. Walker, M. J. Carr, L. C. Patino, O. Matias, and M. D. Feigenson (2003), Flux versus decompression melting at stratovolcanoes in southeastern Guatemala, *J. Volcanol. Geotherm. Res.*, *119*, 21–50, doi:10.1016/S0377-0273(02)00304-9.
- Carr, M. J., M. D. Feigenson, and E. A. Bennett (1990), Incompatible element and isotopic evidence for tectonic control of source mixing and melt extraction along the Central American arc, *Contrib. Mineral. Petrol.*, *105*, 369–380, doi:10.1007/BF00286825.
- Carr, M. J., M. D. Feigenson, L. C. Patino, and J. A. Walker (2003), Volcanism and geochemistry in Central America: Progress and problems, in *Inside the Subduction Factory, Geophys. Monogr. Ser.*, vol. 138, edited by J. Eiler, pp. 153–179, AGU, Washington, D. C.
- Carr, M. J., I. Saginor, G. E. Alvarado, L. L. Bolge, F. N. Lindsay, K. Milidakis, B. D. Turrin, M. D. Feigenson, and C. C. Swisher III (2007a), Element fluxes from the volcanic front of Nicaragua and Costa Rica, *Geochem. Geophys. Geosyst.*, *8*, Q06001, doi:10.1029/2006GC001396.
- Carr, M. J., M. D. Feigenson, and L. C. Patino (2007b), Petrology and geochemistry of lavas, in *Central America: Geology, Resources and Hazards*, edited by J. Bundschuh and G. Alvarado, chap. 22, pp. 565–590, Taylor and Francis, London.
- Chase, C. G. (1972), The N plate problem of plate tectonics, *Geophys. J. R. Astron. Soc.*, *29*, 117–122.
- DeMets, C. (2001), A new estimate for present-day Cocos-Caribbean plate motion: Implications for slip along the Central American volcanic arc, *Geophys. Res. Lett.*, *28*(21), 4043–4046, doi:10.1029/2001GL013518.
- DePaolo, D. (1981), Trace element and isotopic effects of combined wallrock assimilation and fractional crystallization, *Earth Planet. Sci. Lett.*, *53*, 189–202, doi:10.1016/0012-821X(81)90153-9.
- Dollfus, A., and E. Montserrat (1868), *Voyage géologique dans les républiques de Guatemala et de Salvador*, 539 pp., Imprimerie Imp., Paris.
- Eiler, J. M., M. J. Carr, M. Reagan, and E. Stolper (2005), Oxygen isotope constraints on the sources of Central American arc lavas, *Geochem. Geophys. Geosyst.*, *6*, Q07007, doi:10.1029/2004GC000804.
- Feigenson, M. D., and M. J. Carr (1985), Determination of major, trace and rare earth elements in rocks by DCP-AES, *Chem. Geol.*, *51*, 19–27, doi:10.1016/0009-2541(85)90084-1.
- Feigenson, M. D., and M. J. Carr (1993), The source of Central American lavas: Inferences from geochemical inverse modeling, *Contrib. Mineral. Petrol.*, *113*, 226–235, doi:10.1007/BF00283230.
- Feigenson, M. D., M. J. Carr, L. C. Patino, S. Maharaja, and S. Juliano (1996), Isotopic identification of distinct mantle domains beneath Central America, *Geol. Soc. Am. Abstr. Programs*, *28*, 230.
- Feigenson, M. D., M. J. Carr, S. V. Maharaj, S. Juliano, and L. L. Bolge (2004), Lead isotope composition of Central American volcanoes: Influence of the Galapagos plume, *Geochem. Geophys. Geosyst.*, *5*, Q06001, doi:10.1029/2003GC000621.
- Foley, S. (1991), High-pressure stability of the fluor- and hydroxyl-endmembers of pargasite and K-richrichterite, *Geochim. Cosmochim. Acta*, *55*, 2689–2694, doi:10.1016/0016-7037(91)90386-J.
- Geist, D. J., D. J. Fornari, M. D. Kurz, K. S. Harpp, S. A. Soule, M. R. Perfit, and A. M. Koleszar (2006), Submarine Fernandina: Magmatism at the leading edge of the Galápagos hot spot, *Geochem. Geophys. Geosyst.*, *7*, Q12007, doi:10.1029/2006GC001290.
- Gill, J., M. Reagan, F. Tepley, and E. Malavassi (2006), Introduction to special issue: Arenal Volcano, Costa Rica: Magma genesis and volcanological processes, *J. Volcanol. Geotherm. Res.*, *157*, 1–8, doi:10.1016/j.jvolgeores.2006.03.034.
- Girard, G., and B. van Wyk de Vries (2005), The Managua Graben and Las Sierras-Masaya volcanic complex (Nicaragua); pull-apart localization by an intrusive complex: Results from analogue modeling, *J. Volcanol. Geotherm. Res.*, *144*, 37–57, doi:10.1016/j.jvolgeores.2004.11.016.
- Green, T. H. (1995), Significance of Nb/Ta as an indicator of geochemical processes in the crust mantle system, *Chem. Geol.*, *120*, 347–359, doi:10.1016/0009-2541(94)00145-X.
- Green, T. H., and N. J. Pearson (1987), An experimental study of Nb and Ta partitioning between Ti-rich minerals and silicate liquids at high pressure and temperature, *Geochim. Cosmochim. Acta*, *51*, 55–62, doi:10.1016/0016-7037(87)90006-8.
- Hoernle, K., et al. (2008), Arc-parallel flow in the mantle wedge beneath Costa Rica and Nicaragua, *Nature*, *451*(7182), 1094–1097, doi:10.1038/nature06550.
- Kamber, B. S., and K. D. Collerson (2000), Zr/Nb systematic of ocean island basalts reassessed—The case for binary mixing, *J. Petrol.*, *41*(7), 1007–1021, doi:10.1093/ptrology/41.7.1007.
- Kelemen, P. B., G. M. Yogodzinski, and D. W. Scholl (2003), Along-strike variation in the Aleutian Island Arc: Genesis of high Mg# andesite and implications for continental crust. *Inside the Subduction Factory, Geophys. Monogr. Ser.*, vol. 138, edited by J. Eiler, pp. 233–276, AGU, Washington, D. C.
- Klemme, S., J. D. Blundy, and B. J. Wood (2002), Experimental constraints on major and trace element partitioning during partial melting of eclogite, *Geochim. Cosmochim. Acta*, *66*, 3109–3123, doi:10.1016/S0016-7037(02)00859-1.
- Klemme, S., S. Prowatke, K. Hametner, and D. Gunther (2005), Partitioning of trace elements between rutile and silicate melts: Implications for subduction zones, *Geochim. Cosmochim. Acta*, *69*, 2361–2371, doi:10.1016/j.gca.2004.11.015.
- Kurz, M. D., and D. Geist (1999), Dynamics of the Galápagos hotspot from helium isotope geochemistry, *Geochim. Cosmochim. Acta*, *63*, 4139–4156, doi:10.1016/S0016-7037(99)00314-2.



- Kutterolf, S., A. Freundt, W. Peréz, T. Mörz, U. Schacht, H. Wehrmann, and H.-U. Schmincke (2008), Pacific offshore record of plinian arc volcanism in Central America: 1. Along-arc correlations, *Geochem. Geophys. Geosyst.*, *9*, Q02S01, doi:10.1029/2007GC001631.
- Liaw, H. B., and T. Matumoto (1980), Hinge faulting and its correlation with surface geology in northern Costa Rica, *Eos Trans. AGU*, *61*(17), 289–290.
- Lundgren, P., M. Protti, A. Donnellan, M. Heflin, E. Hernandez, and D. Jefferson (1999), Seismic cycle and plate margin deformation in Costa Rica: GPS observations from 1994 to 1997, *J. Geophys. Res.*, *104*(B12), 28,915–28,926, doi:10.1029/1999JB900283.
- Molnar, P., and L. R. Sykes (1969), Tectonics of the Caribbean and Middle America regions from focal mechanisms and seismicity, *Geol. Soc. Am. Bull.*, *80*, 1639–1684, doi:10.1130/0016-7606(1969)80[1639:TOTCAM]2.0.CO;2.
- Münker, C., G. Wörner, G. Yogodzinski, and T. Churikova (2004), Behaviour of high field strength elements in subduction zones: Constraints from Kamchatka-Aleutian arc lavas, *Earth Planet. Sci. Lett.*, *224*(3–4), 275–293, doi:10.1016/j.epsl.2004.05.030.
- Niida, K., and D. H. Green (1999), Stability and chemical composition of pargasite amphibole in MORB pyroxene under upper mantle conditions, *Contrib. Mineral. Petrol.*, *135*, 18–40, doi:10.1007/s004100050495.
- Patino, L. C., M. J. Carr, and M. D. Feigenson (2000), Local and regional variations in Central American arc lavas controlled by variations in subducted sediment input, *Contrib. Mineral. Petrol.*, *138*, 265–283.
- Protti, M., F. Gundel, and K. McNally (1995), Correlation between the age of the subducting Cocos plate and the geometry of the Wadati-Benioff zone under Nicaragua and Costa Rica, *Spec. Pap. Geol. Soc. Am.*, *295*, 309–326.
- Reagan, M. K., and J. B. Gill (1989), Coexisting calcalkaline and high-niobium basalts from Turrialba Volcano, Costa Rica: Implications for residual titanates in arc magma sources, *J. Geophys. Res.*, *94*(B4), 4619–4633, doi:10.1029/JB094iB04p04619.
- Reagan, M. K., J. D. Morris, E. A. Herrstrom, and M. T. Murrell (1994), Uranium series and beryllium isotope evidence for an extended history of subduction modification of the mantle below Nicaragua, *Geochim. Cosmochim. Acta*, *58*(19), 4199–4212, doi:10.1016/0016-7037(94)90273-9.
- Rogers, R. D., H. Karason, and R. D. van der Milt (2002), Epeirogenic uplift above a detached slab in northern Central America, *Geology*, *30*(11), 1031–1034, doi:10.1130/0091-7613(2002)030<1031:EUAADS>2.0.CO;2.
- Saginor, I., E. Gazel, M. Carr, and C. Swisher (2009), Miocene to recent volcanic history of western Nicaragua and the geochemical evolution of the volcanic front, *Geol. Soc. Am. Abstr. Programs*, *41*(4), 54.
- Sapper, K. (1917), *Katalog der Geschichtlichen Vulkanausbrüche*, 358 pp., Karl J Trubner, Strasbourg, France.
- Stoiber, R. E., and M. J. Carr (1973), Quaternary volcanic and tectonic segmentation of Central America, *Bull. Volcanol.*, *37*, 304–325.
- Sun, S. S., and W. F. McDonough (1989), Chemical and isotopic systematics of oceanic basalts: Implications for mantle compositions and processes, in *Magmatism in the Ocean Basins*, edited by A. D. Saunders and M. J. Norry, *Geol. Soc. Spec. Publ.*, *42*, 313–345.
- Syracuse, E. M., and G. A. Abers (2006), Global compilation of variations in slab depth beneath arc volcanoes and implications, *Geochem. Geophys. Geosyst.*, *7*, Q05017, doi:10.1029/2005GC001045.
- Tiepolo, M., R. Vannucci, R. Oberti, S. Foley, P. Bottazzi, and A. Zanetti (2000), Nb and Ta incorporation and fractionation in titanite and kaersutite: Crystal-chemical constraints and implications for natural systems, *Earth Planet. Sci. Lett.*, *176*, 185–201, doi:10.1016/S0012-821X(00)00004-2.
- Tiepolo, M., R. Oberti, and R. Vannucci (2002), Trace-element incorporation in titanite: Constraints from experimentally determined solid/liquid partition coefficients, *Chem. Geol.*, *191*, 105–119, doi:10.1016/S0009-2541(02)00151-1.
- Ui, T. (1972), Recent volcanism in Masaya-Granada area, Nicaragua, *Bull. Volcanol.*, *36*, 174–190, doi:10.1007/BF02596989.
- Vogel, T. A., T. P. Flood, L. C. Patino, M. S. Wilmont, R. P. R. Maximo, C. B. Arpa, C. A. Arcilla, and J. A. Stimac (2006), Geochemistry of silicic magmas in the Macolod Corridor, SW Luzon Philippines: Evidence of distinct, mantle-derived, crustal sources for silicic magmas, *Contrib. Mineral. Petrol.*, *151*, 267–281, doi:10.1007/s00410-005-0050-7.
- Walker, J. A. (1984), Volcanic rocks from the Nejapa and Granada cinder cone alignments, Nicaragua, *J. Petrol.*, *25*, 299–342.
- Woodhead, J., S. Eggins, and J. Gamble (1993), High field strength and transition element systematics in island arc and back-arc basin basalts: Evidence for multi-phase melt extraction and a depleted mantle wedge, *Earth Planet. Sci. Lett.*, *114*, 491–504, doi:10.1016/0012-821X(93)90078-N.
- Xiong, X. L., J. Adam, and T. H. Green (2005), Rutile stability and rutile/melt HFSE partitioning during partial melting of hydrous basalt: Implications for TTG genesis, *Chem. Geol.*, *218*, 339–359, doi:10.1016/j.chemgeo.2005.01.014.